Bottle beam from a bare laser for single-beam trapping

Ching-Hsu Chen, Po-Tse Tai, and Wen-Feng Hsieh

We demonstrate that a laser beam converging from a specific transverse mode is a bottle beam, as described in J. Opt. Soc. Am. B **20,** 1220 (2003). To our knowledge, this is the first time that a bottle beam has been generated directly from a laser. By calculating the radiation forces on a dielectric Rayleigh sphere in the bottle beam, we show that the single beam can trap high-refractive-index particles at the multiple axial sites of intensity maxima, and it can confine low-index particles on a transverse plane within the bottle regions. Such a novel laser beam may have other applications. © 2004 Optical Society of America

OCIS codes: 140.0140, 140.7010, 140.3580, 140.3480.

1. Introduction

A single-beam optical trap known as optical tweezers[1] has become an important tool in many fields. Besides the fundamental Gaussian beam, many kinds of optical beams have been studied to trap particles. Recently a Bessel beam, acting as inverted tweezers, has been developed to manipulate particles in multiple axial sites based on its property of self-reconstruction.[2] However, such a beam does not allow true trapping three dimensionally because the Bessel beam achieves only two-dimensional confinement in transverse planes. On the other hand, an optical dark region that is surrounded by light in all directions was created by using a wave plate and was used by Ozeri *et al.*[3] to trap atoms. Such a dark volume was later called an optical bottle,[4] which one can construct from the interference of Laguerre–Gaussian, LG_{00} and LG_{20}, modes by using a computer-generated hologram outside the cavity. The bottle beam has an obvious application for trapping particles with a refractive index lower than the surrounding medium. However, the two axial sites of highest intensity beside the bottle region may be used to trap simultaneously high-refractive-index particles and may become true three-dimensional tweezers in multiple axial sites.

Lately we have observed a multi-beam-waist (MBW) mode[5] that possesses more than one intensity maximum in an end-pumped Nd:YVO_4 laser with degenerate cavities when the pump radius is smaller than the fundamental mode radius. We have verified the MBW mode by using the Collins integral together with rate equations and understand it by using a combination picture of the ray and wave optics.[5] The MBW mode generated with a cavity of $g_1g_2 = 1/4$ possesses three intensity maxima after being condensed by a convergent lens. We demonstrate here that the MBW mode is in fact a bottle beam because of the constructive interference of LG_{p0} modes near the focus with a radial index of $p = 0, 3, 6, \ldots$, and an angular index of zero. As far as we know, this is the first time that a bottle beam has been generated directly from a laser. Such a bottle beam with intensity maxima near the focus may have the potential to achieve three-dimensional trapping at the multiple axial sites of the intensity maxima.

It is known that treating the interaction of an incident Gaussian beam with a dielectric scatterer requires the generalized Lorenz–Mie theory.[6,7] However, dealing with the problem for a weakly convergent Gaussian beam illuminating a Rayleigh particle is relatively simple and has been demonstrated to be consistent with the generalized Lorenz–Mie theory.[8] Although the Rayleigh approximation is valid only for particles that are sufficiently smaller than the wavelength of light, a necessary condition for single-beam axial trapping, that the axial component of the gradient force must be larger than the scattering force, can be determined by this approach. Besides, calculation of a weakly convergent beam is useful in the application of laser guidance.[9] By calculating the radiation forces on a dielectric Rayleigh sphere under the

C.-H. Chen is with the National Center for High-Performance Computing, 21 Nan-ke Third Road, Hsin-shi, Tainan County 744, Taiwan. P.-T. Tai and W.-F. Hsieh (wfhsieh@mail.nctu.edu.tw) are with the Department of Photonics and Institute of Electro-Optical Engineering, National Chiao Tung University, 1001 Tahsueh Road, Hsinchu 30050, Taiwan.

Received 16 February 2004; revised manuscript received 5 August 2004; accepted 9 August 2004.

0003-6935/04/326001-06$15.00/0

illumination of a weakly convergent bottle beam from a bare laser with $g_1g_2 = 1/4$, we show that the gradient force is larger than those for the fundamental Gaussian beam with the same trapping power and waist radius. Therefore we believe that the single bottle beam that we are discussing is able to trap the high-index particles at the multiple axial sites of the intensity maxima. Moreover the beam can confine low-index particles in the transverse plane within the bottle regions, so that it can be used as inverted tweezers as the Bessel beam[2] was for high-index particles. Note that the beam used in the force calculation does not have a perfect bottle but only an ~50% contrast (the ratio of the on-axis intensity to the off-axis peak intensity) in the depth of the bottle, which is the result of our mode calculation with a 1-mm aperture radius at the flat end of the mirror. When we insert a hard aperture inside the cavity with a pump radius of 30 μm we experimentally obtain a 7% contrast in the bottle regions. Our mode calculation shows that the contrast in the bottle can be reduced to 1% by using a smaller pump size and a proper aperture.

In Section 2 we describe the equations of radiation forces for a Rayleigh sphere under the illumination of the weakly convergent bottle beam. In Section 3 we show first that the bottle beam from a bare laser can be expanded into the superposition of LG modes, and then we show the calculating results of radiation forces. Finally in Section 4 we discuss the conclusions.

2. Model

Because the bottle beam from a bare laser can be expanded into a linear combination of the LG_{p0} modes, the electric-field vector and the magnetic-field vector for a linearly polarized bottle beam can be written in mks units as

$$\mathbf{E}(\mathbf{r}, t) = \mathrm{Re}\left[\sum_p E_{p0}(\mathbf{r})\exp(-i\omega t)\right]\mathbf{i} = \mathrm{Re}[E_{\mathrm{BBL}}(\mathbf{r})\exp(-i\omega t)]\mathbf{i}, \quad (1)$$

$$\mathbf{H}(\mathbf{r}, t) \cong \mathbf{k} \times \frac{\mathbf{E}(\mathbf{r}, t)}{Z} = n_2\varepsilon_0 c\ \mathrm{Re}[E_{\mathrm{BBL}}(\mathbf{r})\exp(-i\omega t)]\mathbf{j} = \mathrm{Re}[H_{\mathrm{BBL}}(\mathbf{r})\exp(-i\omega t)]\mathbf{j}, \quad (2)$$

where the subscript BBL is the bottle-beam laser, $\mathbf{r}$ is the position vector of the particle, Re is the real part of a complex quantity, ω is the optical frequency, $\mathbf{i}$ is the unit vector in the polarized direction of the electric field, $\mathbf{k}$ is the unit vector in the beam propagation direction, $Z = (\mu_2/\varepsilon_2)^{1/2} = [\mu_0/(\varepsilon_0 n_2{}^2)]^{1/2}$ is the impedance of the nonconducting and nonmagnetic surrounding medium, n_2 is the refractive index of the medium, c is the velocity of light in vacuum, μ_0 and ϵ_0 are the magnetic permeability and the dielectric constant in vacuum, respectively. Note that the field descriptions of the LG modes are merely a paraxial approximation of the scalar wave equation. The intensity distribution can be written as

$$I(\mathbf{r}) \equiv \langle \mathbf{S}(\mathbf{r}, t)\rangle_T = \frac{1}{2}\mathrm{Re}[E_{\mathrm{BBL}}(\mathbf{r}) \times H_{\mathrm{BBL}}{}^*(\mathbf{r})] = \frac{n_2\varepsilon_0 c}{2}|E_{\mathrm{BBL}}(\mathbf{r})|^2\mathbf{k}, \quad (3)$$

where $\mathbf{S}$ is the Poynting vector of the paraxial beam and $\langle\ \rangle_T$ represents the time average.

Consider that a single nonmagnetic dielectric spherical particle is illuminated by a paraxial beam of linearly polarized light. If the particle is sufficiently smaller than the wavelength of the incident light, the particle is polarized as in the uniform field. The dipole moment is given by[10]

$$\mathbf{p}(\mathbf{r}, t) = 4\pi n_2{}^2\varepsilon_0 a^3\left(\frac{n_r{}^2 - 1}{n_r{}^2 + 2}\right)\mathbf{E}(\mathbf{r}, t), \quad (4)$$

where a is the particle radius, $n_r = n_1/n_2$, and n_1 is the refractive index of the particle. According to Ref. 8, the forces acting on a Rayleigh particle can be divided into two types, the scattering force and the gradient force. The scattered wave radiates in all directions from the dipole particle and changes the direction of the energy flux in the system, imparting a momentum change in the particle. The scattering force is given by[10]

$$\mathbf{F}_{\mathrm{scat}}(\mathbf{r}) = \frac{n_2}{c}C_{pr}I(\mathbf{r})\mathbf{k} = \frac{n_2}{c}\frac{8}{3}\pi k^4 a^6\left(\frac{n_r{}^2 - 1}{n_r{}^2 + 2}\right)^2 I(\mathbf{r})\mathbf{k}, \quad (5)$$

where C_{pr} is the scattering cross section of the particle and k is the wave number. The gradient force coming from the Lorenz force of the induced dipole in the electromagnetic field is written as[10]

$$\mathbf{F}_{\mathrm{grad}}(\mathbf{r}) = \langle[\mathbf{p}(\mathbf{r}, t)\ \cdot\ \nabla]\mathbf{E}(\mathbf{r}, t)\rangle_T = \frac{2\pi n_2 a^3}{c}\left(\frac{n_r{}^2 - 1}{n_r{}^2 + 2}\right)\nabla I(\mathbf{r})\mathbf{k}. \quad (6)$$

To exhibit the radiation forces clearly, we assume a high-index particle with a radius $a = 20$ nm in the Rayleigh regime[10]: $a < \lambda/20$ with $n_1 = 1.45$ in air ($n_2 = 1$) as in the experimental situation in Ref. 11. With cylindrical symmetry the radial and the axial components of ∇I in Eq. (6) are $\mathrm{d}I/\mathrm{d}\rho$ and $\mathrm{d}I/\mathrm{d}z$, respectively. We set $\mathrm{d}z = \mathrm{d}\rho \sim 0.488$ μm as the increments between two successive data points in our simulation of the mode calculation.[5]

3. Results

The MBW mode at a 1.064-μm wavelength has been observed in an end-pumped Nd:YVO_4 laser with a simple plano–concave cavity of $g_1g_2 = 1/4$.[5] The simulated mode pattern along the propagation distance is shown in Fig. 1(a) for a cavity length of 60 mm, a pump radius of 30 μm, an effective pump power of 100 mW, an aperture radius of 1 mm at the flat end

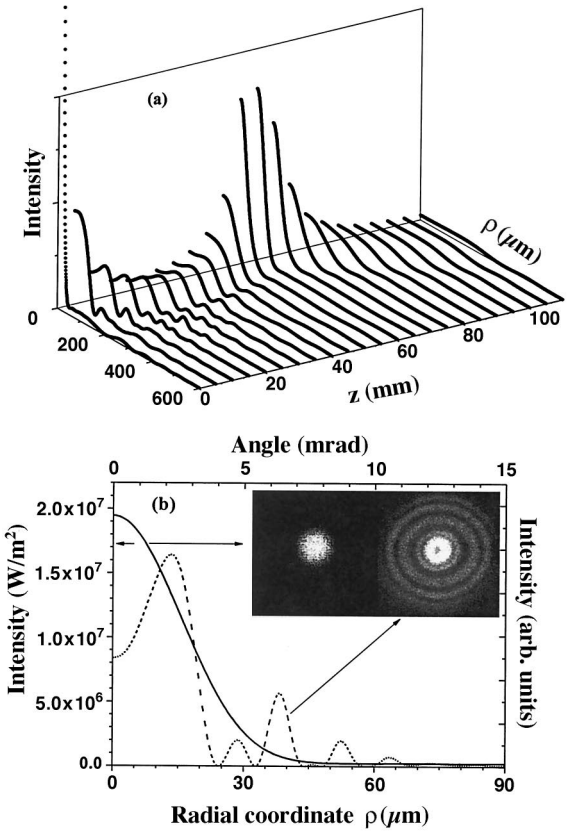

Fig. 1. (a) Numerical profile variation of the MBW mode. (b) Mode patterns at the flat mirror end (solid curve with the bottom and left scale) and in the far field (dashed curve with the top and the right scale) together with experimental photographs. The speckles in the photographs are due to screen reflection. The fitted coefficients for the solid curve are $\eta_0 = 1$, $\eta_3 = 0.82$, $\eta_6 = 0.66$, $\eta_9 = 0.41$, $\eta_{12} = 0.35$, $\eta_{15} = 0.22$, $\eta_{18} = 0.08$, $\eta_{21} = 0.08$.

of the mirror, and a 90% transmittance of the output coupler (the curved mirror). Note that $z = 0$ mm in Fig. 1(a) denotes the axial position of the flat end of the mirror (the dichroic-coated face of the Nd:YVO_4 crystal), and $z < 60$ mm is within the cavity. Figure 1(b) shows that the numerical near-field pattern at $z = 0$ has a near-Gaussian profile with a much smaller waist radius of 30.3 μm than the fundamental eigenmode of $w_c = 108$ μm, whereas the far-field pattern has concentric rings with a dark center, which agrees quite well with the experiment [see the photographs in Fig. 1(b)]. Since the observed profiles are cylindrically symmetric, we fitted the near-field profile by using the degenerate LG mode expansion. The electric field of a LG_{pm} mode with an angular index $m = 0$ can be expressed as

$$E_{p0}(\rho, z) = A_{p0}(\rho, z)\exp\left[-\frac{\rho^2}{w(z)^2}\right] \times \exp\left[i\frac{k\rho^2}{2R(z)}\right]\exp\left\{i\left[kz - (2p + 1)\tan^{-1}\left(\frac{z}{z_R}\right)\right]\right\},$$

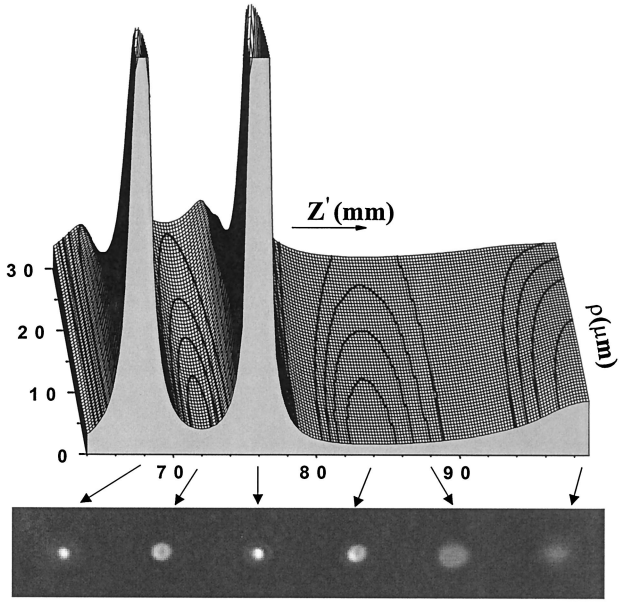

Fig. 2. Bottle beam condensed from the MBW mode through a convergent lens with a focal length of 52 mm at a distance of 105 mm from the output coupler. The three high-intensity extrema are at $Z' = 68$, 76, 100 mm, and the bottle centers are at $Z' = 72$, 84 mm. The calculated beam profiles point to the experimental photographs.

where

$$A_{p0}(\rho, z) = E_0 \frac{w_c}{w(z)} L_p{}^0\left[\frac{2\rho^2}{w(z)^2}\right]$$

is the modal function, z_R is the Rayleigh length; $w(z)$ is the beam radius; $R(z)$ is the radius of curvature of the phase front; ρ and z are, respectively, the radial and the axial coordinates; and $L_p{}^0(\rho, z)$ is the Laguerre polynomial for the mode index p. We assume that all the excited cavity eigenmodes have the same wave number and are in phase at $z = 0$; thus we can use $|\eta_0 E_{00} + \eta_3 E_{30} + \cdots + \eta_{21} E_{21,0}|^2$ to fit the mode profile, where E_{p0} are the normalized field, η_0 is fixed unity, and the η terms (real coefficients) are mode weight ratios to E_{00}. The fitted profile was normalized with respect to the central peak intensity of the mode-calculation solution.

The fitted result overlaps with the profile in Fig. 1(b) with $\eta_3 = 0.82$, $\eta_6 = 0.66$, . . . , as listed in the Fig. 1(b) caption. We associated the Gouy phase shifts with every one of the cavity eigenmodes and made the profile variation with z almost the same as in Fig. 1(a). The waist at $z = 0$ and the intensity maximum at $z = \sqrt{3}z_R \sim 60$ mm are due to being in phase among these degenerate modes, whereas the local minimum at $z \sim z_R/\sqrt{3} = 2$ cm in Fig. 1(a) as well as the far-field profile in Fig. 1(b) is due mainly to being out of phase between the LG_{00} and LG_{30} modes. When the beam was propagated through a convergent lens, three intensity maxima and two optical bottles were obtained as shown in Fig. 2, where the thick black curves are the intensity contours and

$Z' = 0$ mm denotes the axial position of the convergent lens. This combination of phase-locked LG modes forms an optical bottle beam in spite of the nonzero local minimum of the axial intensity. Note that the bottle beam of Ref. 4 has only two intensity maxima. As far as we know, this is the first time that a bottle beam has been generated directly from a bare laser. This laser has the following characteristics:

(1) It is simple and compact and needs only a convergent lens outside the laser cavity.
(2) More than 300 mW of output is available, which can be further increased with a longer cavity and larger pump size.
(3) The locations of the intensity maxima can be adjusted according to the Gaussian lens law as with the ray geometry in Fig. 4 of Ref. 5.
(4) The depth of the optical bottle may be reduced by inserting an aperture inside the cavity to eliminate the higher-order modes, e.g., the LG_{60} mode, or by modifying the pump beam to control the chosen modes.
(5) Other degenerate cavity configurations supporting the MBW modes can be used, i.e., $g_1 g_2 = 3/4$.

According to characteristic (4) of the laser, we are able to reduce the contrast in the bottle from 50% to 7% by simply inserting a hard aperture with a radius of 350 μm inside the cavity but using the same pump radius of 30 μm as in Fig. 1(b). The experimental result is shown in Fig. 3(a). Because the LG_{60} mode undergoes large diffraction losses for an aperture radius of 350 μm, we compare the profile in Fig. 3(a) with the bottle in Fig. 3(b) that is numerically superimposed from the LG_{00} and LG_{30} modes with a π-phase difference but equal mode weighting. Except for the nonperfect bottle center of Fig. 3(a), the similarity between Figs. 3(a) and 3(b) means that the mode purity indeed shows good improvement when a proper aperture is used. The nonperfect bottle is a result of nonequal mode weighting. However, we may further decrease the pump radius to improve the depth of the bottle. The simulation results in Fig. 3(c) show that the contrast in the bottle can be reduced from 8% to 1% when the pump radius is decreased from 30 μm (solid curve) to 15 μm (dashed curve) while a 350-μm aperture radius is maintained. Decreasing the pump size leads to the mode weight ratio η_3 approaching unity, which means that mode weighting can be controlled by pump size. Note that the simulation in Fig. 3(c) for the case of a 30-μm pump radius agrees very well with the experiment in Fig. 3(a). The small deviation in the contrast between the experiment and the simulation may come from the pump-size measurement. Therefore we believe that the bottle beam from a bare laser provides another choice for optical trapping application, although there are other methods for generating the bottle beam, such as a spatial light modulator and axicons.

The field distribution used in the following is the result of mode calculation for the parameters in Fig. 1. Note that the nonperfect bottle beam exhibits a 50% contrast in the depth of the bottle. We assumed a convergent lens with a focal length of 10 mm at a distance of 25 mm behind the output coupler to focus the bottle beam such that the first intensity maximum has a beam radius $w_0 = 4.9$ μm and the second maximum has $w_0 = 4.0$ μm. The near-Gaussian profile at the first and the second maximum has an on-axis intensity of 7.4×10^8 and 1.1×10^9 W/m^2, respectively, for the same trapping laser power $P = 28.1$ mW. Note that the on-axis intensity equals $2P/(\pi w_0^2)$ for both intensity maxima. So we compare the trapping forces with the Gaussian case with the same trapping power and waist radius. Figure 4(a) shows that the scattering force F_{scat} is always positive in the direction of beam propagation with the maxima at the two intensity maxima of $Z' = 10.74$ and 11.33 mm. However, the axial component of the gradient force $F_{\text{grad},z}$ reverses its direction as it passes the intensity maxima, and the maximal value of the negative $F_{\text{grad},z}$ is larger than the scattering force and thus provides enough force to drag the particle back to the centers of the intensity maxima. Moreover the maximal negative $F_{\text{grad},z} = -5.6 \times 10^{-7}$ and -9.6×10^{-7} pN at the two intensity maxima is larger than the respectively compared Gaussian case for which the maximal negative $F_{\text{grad},z} = -3.1 \times 10^{-7}$ and -6.9×10^{-7} pN. Because the gradient force is less sensitive (3 orders of magnitude)

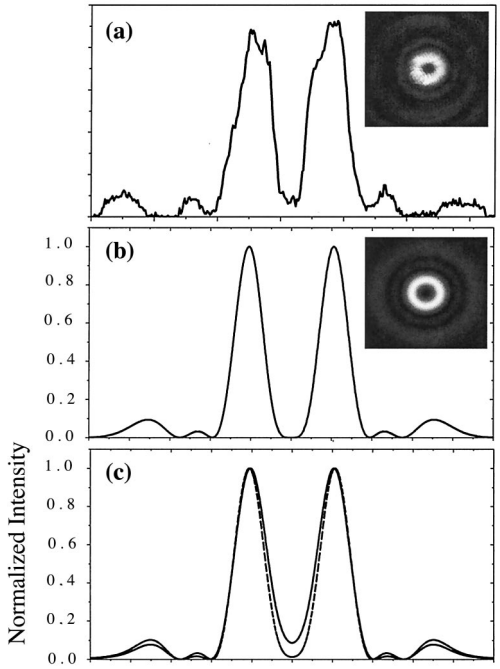

Fig. 3. (a) Experimental result of an optical bottle with a 7% contrast. (b) Simulated bottle with the superimposition of the LG_{00} and LG_{30} modes with equal mode weighting. (c) Two transverse profiles of the optical bottles in mode calculation with an aperture radius of 350 μm and a pump radius of, solid curve, 30 μm and, dashed curve, 15 μm.

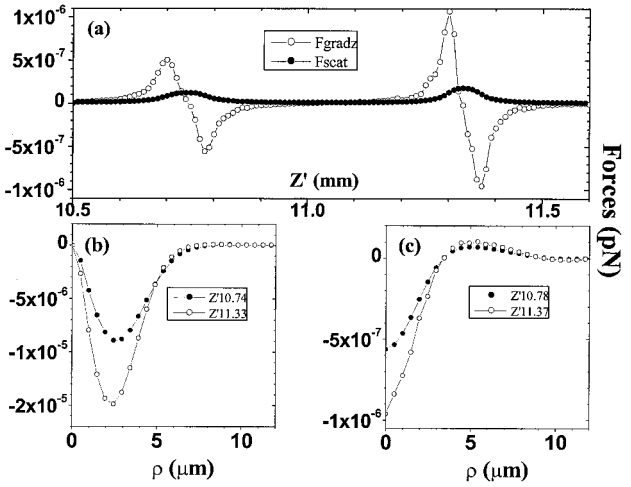

Fig. 4. (a) F_{scat} and $F_{grad,z}$ as a function of the propagation distance. (b) $F_{grad,\rho}$ versus ρ at the positions of the intensity maxima. (c) $F_{grad,z}$ versus ρ at the positions of maximal negative $F_{grad,z}(\rho = 0)$ near the two intensity maxima.

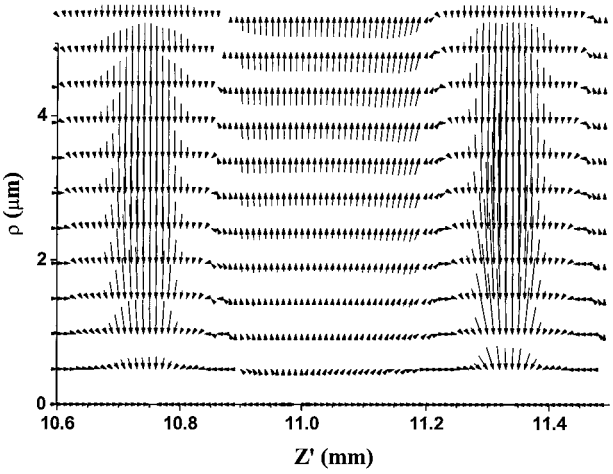

Fig. 5. Vector plots of the total radiation force. The vectors are lengthened 10 times to $Z' = 10.9$–11.2 mm.

to the particle radius than the scattering force, the necessary condition for the single-beam axial trap,

$$\left|\frac{F_{grad,z}(Z_{max}')}{F_{scat}(Z_{max}')}\right| > 1,$$

is satisfied only if the particle radius is smaller than 38 and 42 nm for the first and the second intensity maximum, respectively. Z_{max}' is the position where $F_{grad,z}$ is at a maximum. Figure 4(b) shows that the radial component of the gradient force $F_{grad,\rho}$ always tends to push the sphere to the beam axis and that the maximal negative $F_{grad,\rho}$ occurring at $\sim w_0/2$ is much larger than the maximal negative $F_{grad,z}$. Figure 4(c) shows $F_{grad,z}$ versus ρ for $Z' = 10.78$ and 11.37 mm where the maximal negative $F_{grad,z}(\rho = 0)$ occurs at a distance of ~40 μm from the centers of intensity maxima. The curves in Fig. 4(c) are similar to those of the compared Gaussian case for $w_0 = 4.9$ μm whose maximal negative $F_{grad,z}$ occurs at a distance of $kw_0^2/(2\sqrt{3}) = 41$ μm from its waist center.

In Fig. 4 we see that the radiation forces for both intensity maxima are very similar to the case of the Gaussian beam.[7] Because of the similarity, the necessary and sufficient condition for a stable axial trap, $U > 10k_BT$, was used to estimate the lower limit of the particle radius as was done in Refs. 1 and 8, where U is the potential of the gradient force, k_B is the Boltzman constant, and T is the absolute temperature. Assuming a trapping power of 281 mW and $w_0 = 1$ μm at $T = 293$ K, the criterion gives a lower limit of $a = 34$ nm. The lower limit obtained is indeed smaller than the upper limit estimated from the necessary condition mentioned above. Therefore this bottle beam is able to trap high-index particles with tens of nanometers at the two sites of the intensity maxima.

The total radiation force, the vector sum of the scattering force and the gradient force, is plotted as vectors in Fig. 5. The total force traps the high-index sphere near the intensity maxima while the arrows point away from $(\rho, Z') = (0, 11.0$ mm) for the bottle region of $Z' = 10.9$–11.2 mm. Because the gradient force is dominant in Fig. 4(a), the force vector will reverse the directions of the arrows in Fig. 5 when $(n_r^2 - 1)/(n_r^2 + 2)$ in Eq. (6) becomes negative for a low-index particle of $n_r < 1$ such as a bubble in the liquid. Although $F_{grad,z}$ on a low-index particle is very weak near the bottle region, $F_{grad,\rho}$ is approximately equal to 10^{-7} pN for $n_r = 0.75$, which can achieve a two-dimensional confinement in transverse plane. The transversal force $F_{grad,\rho}$ is larger for a deeper bottle. This indicates that the upward bottle beam can be used as inverted tweezers for low-index particles in the two bottle regions as the Bessel beam[2] confines the high-index particles.

Note that the beam used in the calculation is weakly convergent; thus the calculated forces in Figs. 4 and 5 are weak, and the bottle extends more than 300 μm (the distance between two intensity maxima) with a large radius. The forces can be improved when a strongly convergent lens is used, since the aspect ratio z_R/w_0 of the optical bottle changes with the degree of beam convergence.[4] Theoretically the rate of change of the Gouy phase leads to the bottle size of the beam in Fig. 1(a) being smaller than that of the interference from the LG_{00} and the LG_{20} modes. For the practical application of optical tweezers, the trapping beam must be expanded to a millimeter-size range and then focused through an objective lens with a high numerical aperture. Finally we must remember that the calculating model with a paraxial approximation contains errors, depending on $1/(kw_0)$,[12] and thus does not give the correct values of the forces for a strongly convergent beam. The electric and the magnetic field beyond the paraxial approximation should be taken into account for optical tweezers.

4. Conclusions

We have shown that a bottle beam can be directly generated from an end-pumped Nd:YVO_4 laser. With illumination from a weakly convergent bottle beam from a bare laser where $g_1g_2 = 1/4$, the radiation forces on a Rayleigh particle are calculated and the necessary condition for single-beam axial trapping has been found to be satisfactory. We believe that the downward bottle beam can be used as optical tweezers for high-index particles at multiple-intensity maxima. In addition the upward bottle beam can be used as inverted tweezers for low-index particles in the bottle regions. Such a laser beam may be useful for various applications.

The research was partially supported by the National Science Council (NSC) of the Republic of China under grant NSC93-2112-M-009-035. C. H. Chen and P. T. Tai gratefully acknowledge the NSC for providing a fellowship.

References

1. A. Ashkin, J. M. Dziedzic, J. E. Bjorkholm, and S. Chu, "Observation of a single-beam gradient force optical trap for dielectric particles," Opt. Lett. **10,** 288–290 (1986).
2. V. Garces-Chavez, D. McGloin, H. Melville, W. Sibbett, and K. Dholakia, "Simultaneous manipulation in multiple planes using a self-reconstructing light beam," Nature (London) **419,** 145–147 (2002).
3. R. Ozeri, L. Khaykovich, and N. Davidson, "Long spin relaxation times in a single-beam blue-detuned optical trap," Phys. Rev. A **59,** R1750–R1753 (1999).
4. J. Arlt and M. J. Padgett, "Generation of a beam with a dark focus surrounded by regions of higher intensity: the optical bottle beam," Opt. Lett. **25,** 191–193 (2000).
5. C. H. Chen, P. T. Tai, M. D. Wei, and W. F. Hsieh, "Multibeam-waist modes in an end-pumped Nd:YVO_4 laser," J. Opt. Soc. Am. B **20,** 1220–1226 (2003).
6. G. Gouesbet, B. Maheu, and G. Grehan, "Light scattering from a sphere arbitrarily located in a Gaussian beam, using a Bromwich formulation," J. Opt. Soc. Am. B **5,** 1427–1443 (1988).
7. J. P. Barton, D. R. Alexander, and S. A. Schaub, "Theoretical determination of net radiation force and torque for a spherical particle illuminated by a focused laser beam," J. Appl. Phys. **66,** 4594–4602 (1989).
8. Y. Harada and T. Asakura, "Radiation forces on a dielectric sphere in the Rayleigh scattering regime," Opt. Commun. **124,** 529–541 (1996).
9. Y. K. Nahmias and D. J. Odde, "Analysis of radiation forces in laser trapping and laser-guided direct writing applications," IEEE J. Quantum Electron. **38,** 131–141 (2002).
10. J. A. Stratton, *Electromagnetic Theory* (McGraw-Hill, New York, 1941).
11. R. Omori, T. Kobayashi, and A. Suzuki, "Observation of single-beam gradient-force optical trap for dielectric particles in air," Opt. Lett. **22,** 816–818 (1997).
12. L. W. Davis, "Theory of electromagnetic beams," Phys. Rev. A **19,** 1177–1179 (1979).